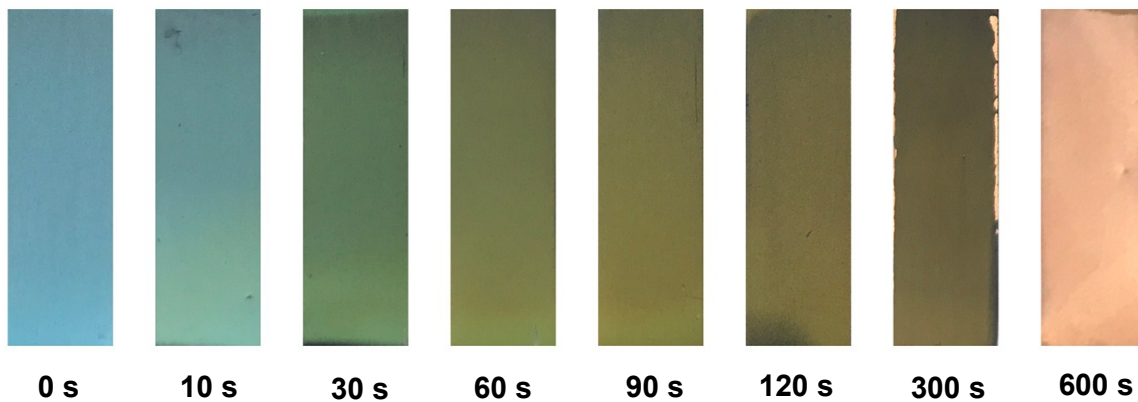


# Hierarchically structured multi-shell nanotube arrays by self-assembly for efficient water oxidation

Steffen Czioska,<sup>1</sup> Jianying Wang,<sup>1</sup> Xue Teng,<sup>1</sup> Shanghshang Zuo,<sup>1</sup> Songhai Xie,<sup>2</sup> Zuofeng Chen\*,<sup>1</sup>

<sup>1</sup>Shanghai Key Lab of Chemical Assessment and Sustainability, School of Chemical Science and Engineering, Tongji University, Shanghai 200092, China; <sup>2</sup>Department of Chemistry, Fudan University, Shanghai 200433, China.



**Figure S1.** Camera pictures of Cu(OH)<sub>2</sub> NWs after immersion in 10 mM Fe<sup>3+</sup> solution for different times. (Fe:Cu(OH)<sub>2</sub> NTs with different contents of iron). The electrode color changes from blue (0 s) over green (30 s) to dark yellow (90 s); beyond that, the nanowires peel off from the copper foil surface (600 s).

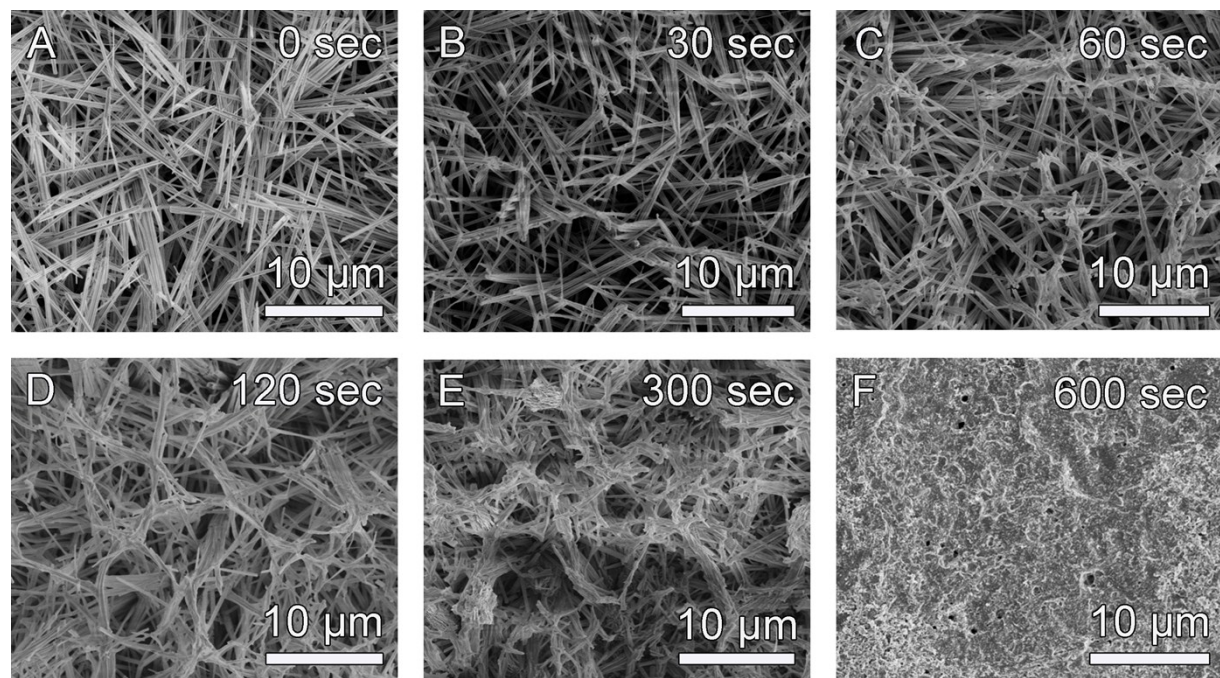


**Figure S2.** SEM images of  $\text{Cu}(\text{OH})_2$  NWs after immersion in 10 mM  $\text{Fe}^{3+}$  solution for different times. (Fe: $\text{Cu}(\text{OH})_2$  NTs with different contents of iron).

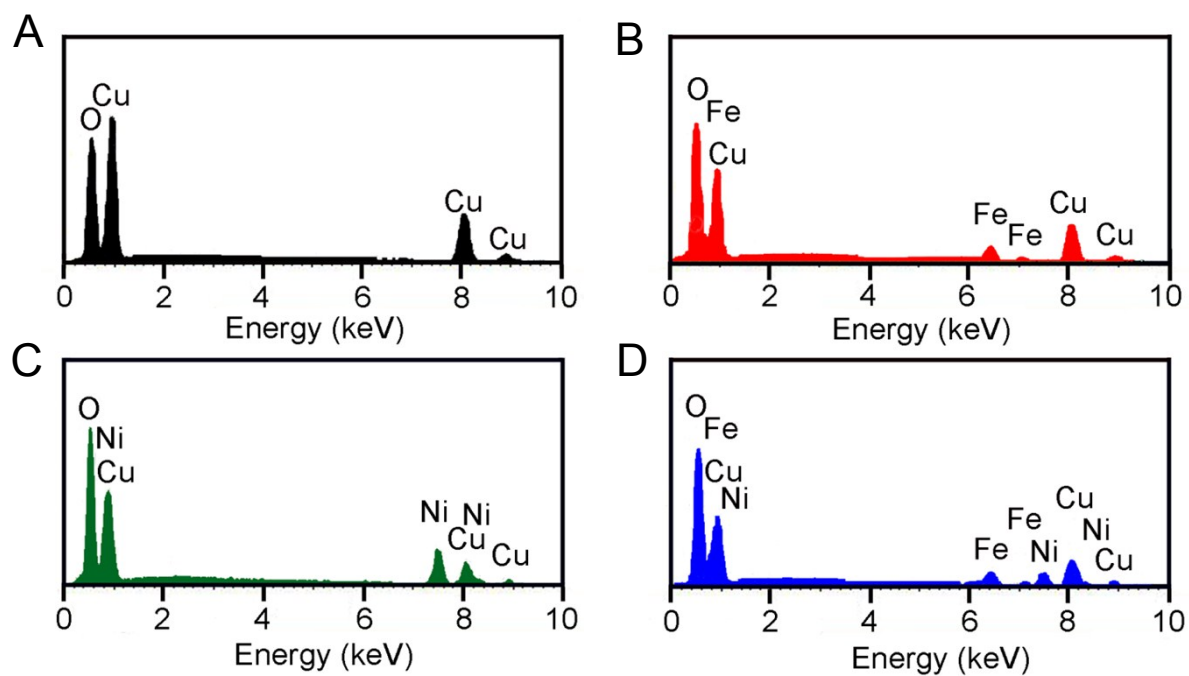


**Figure S3.** EDX of  $\text{Cu}(\text{OH})_2$  NWs (A),  $\text{Fe}:\text{Cu}(\text{OH})_2$  NTs (B),  $\text{Ni}:\text{Cu}(\text{OH})_2$  NWs (C) and  $\text{Ni}:\text{Fe}:\text{Cu}(\text{OH})_2$  NTs (D).

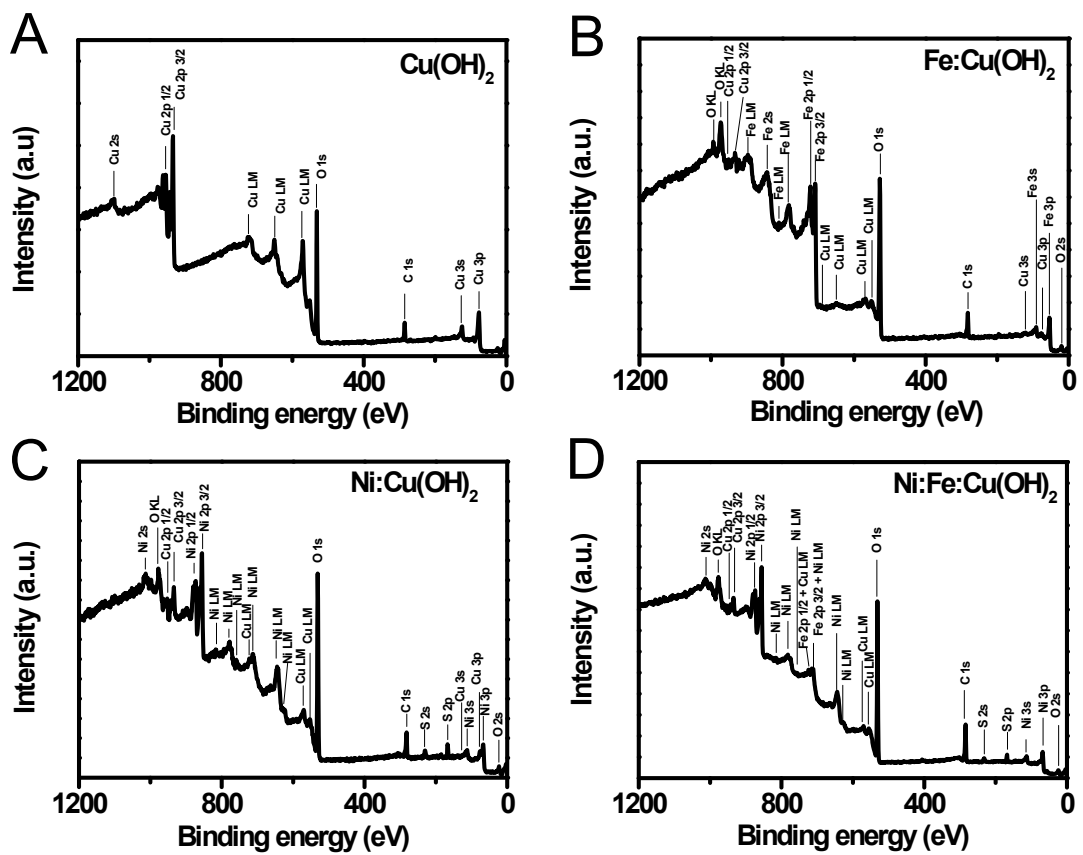


**Figure S4.** Survey XPS of Cu(OH)<sub>2</sub> NWs (A), Fe:Cu(OH)<sub>2</sub> NTs (B), Ni:Cu(OH)<sub>2</sub> NWs (C) and Ni:Fe:Cu(OH)<sub>2</sub> NTs.

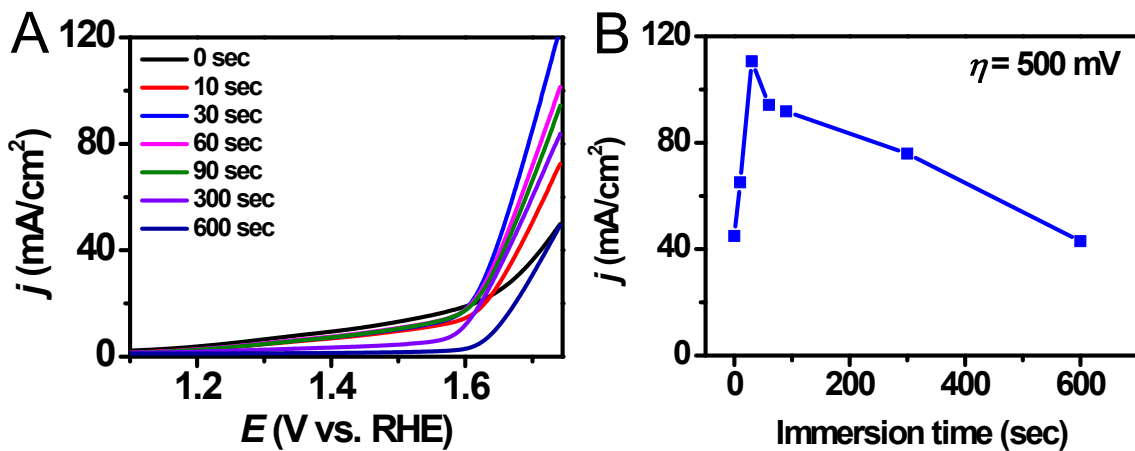


**Figure S5.** Optimization of Fe:Cu(OH)<sub>2</sub> NTs towards the immersion time of Cu(OH)<sub>2</sub> NWs into Fe<sup>3+</sup> solution. LSV curves (A) and summarized current density vs. the immersion time at an overpotential of 500 mV (B). All electrochemical measurements were carried out in 1 M KOH at a scan rate of 20 mV/s with *iR* compensation.

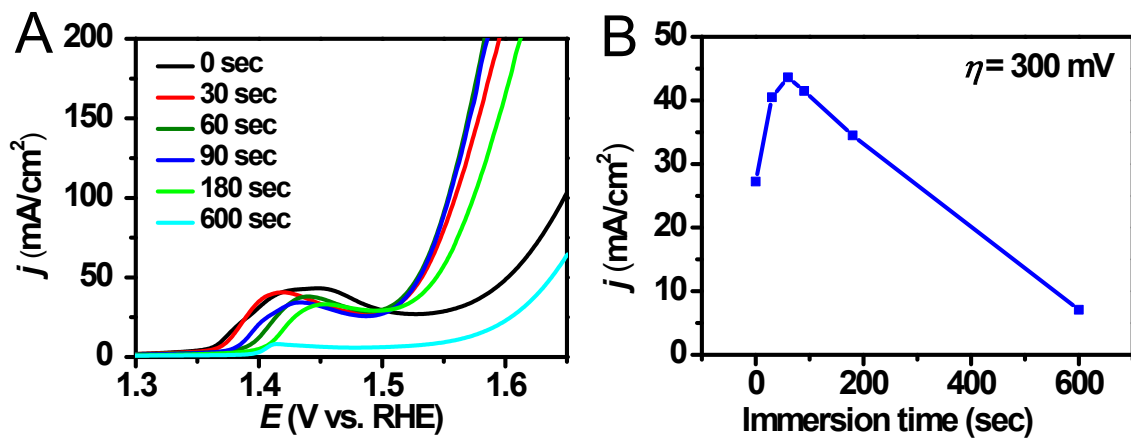


**Figure S6.** Optimization of Ni:Fe:Cu(OH)<sub>2</sub> NTs towards the immersion time of Cu(OH)<sub>2</sub> NWs into Fe<sup>3+</sup> solution. All samples were put into the nickel chemical bath for 20 min afterwards. LSV curves (A) and summarized current density vs. the immersion time at an overpotential of 300 mV (B). All electrochemical measurements were carried out in 1 M KOH at a scan rate of 20 mV/s with *iR* compensation.

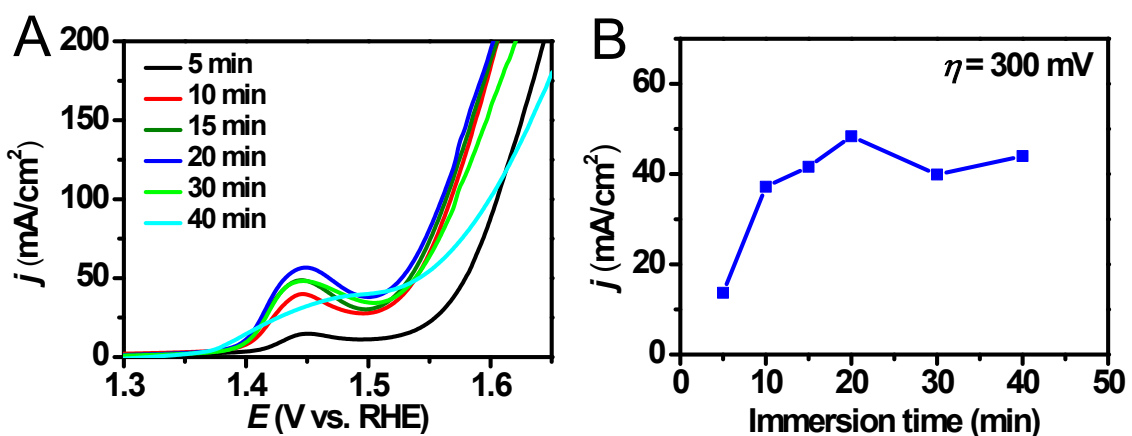


**Figure S7.** Optimization of Ni:Fe:Cu(OH)<sub>2</sub> NTs towards the immersion time of Fe:Cu(OH)<sub>2</sub> into the nickel chemical bath. LSV curves (A) and current density vs. immersion time at an overpotential of 300 mV (B). All electrochemical measurements were carried out in 1 M KOH at a scan rate of 20 mV/s with *iR* compensation.

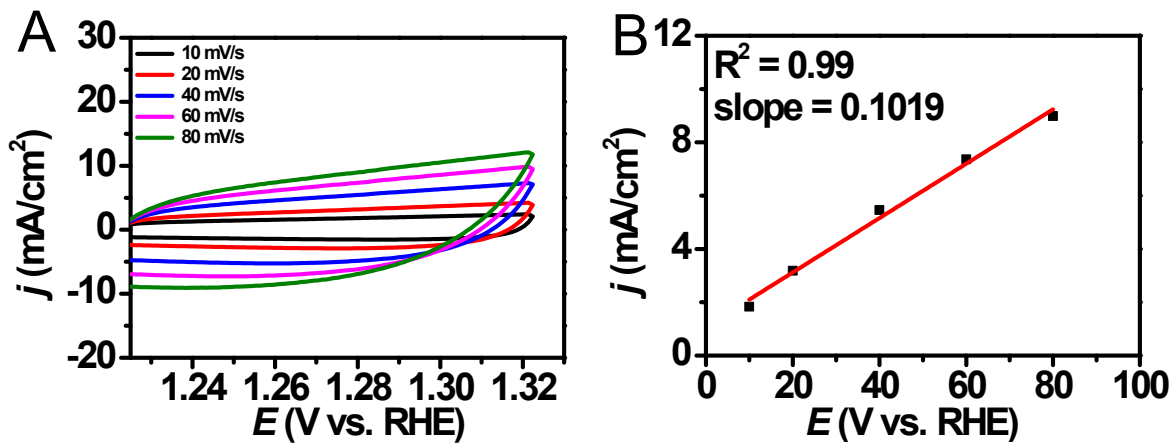


**Figure S8.** Double layer charging capacitance measurements for determination of the electrochemically active surface area of Fe:Cu(OH)<sub>2</sub> NTs in 1 M KOH.

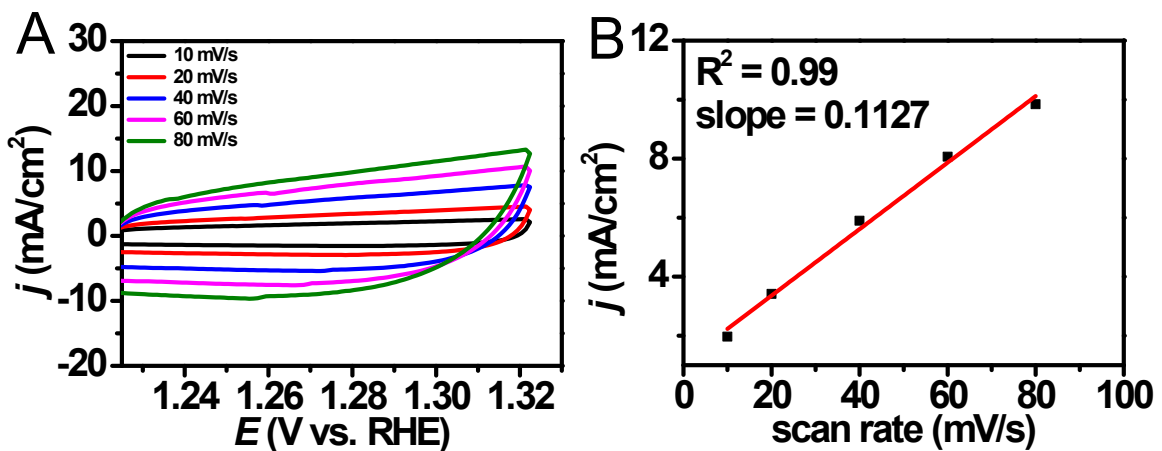


**Figure S9.** Double layer charging capacitance measurements for determination of the electrochemically active surface area of a Ni:Fe: $\text{Cu}(\text{OH})_2$  NTs in 1 M KOH.

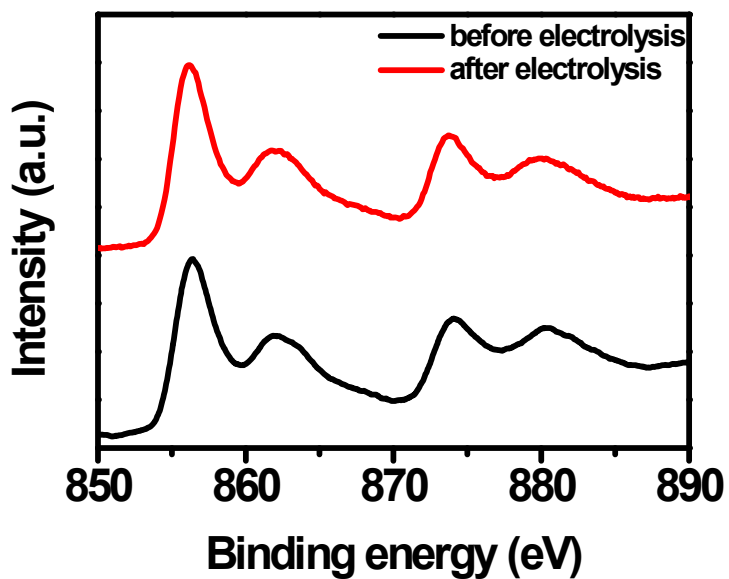


**Figure S10.** XPS of the Ni 2p peaks of Ni:Fe:Cu(OH)<sub>2</sub> NTs before (black) and after (red) 40 h electrolysis.

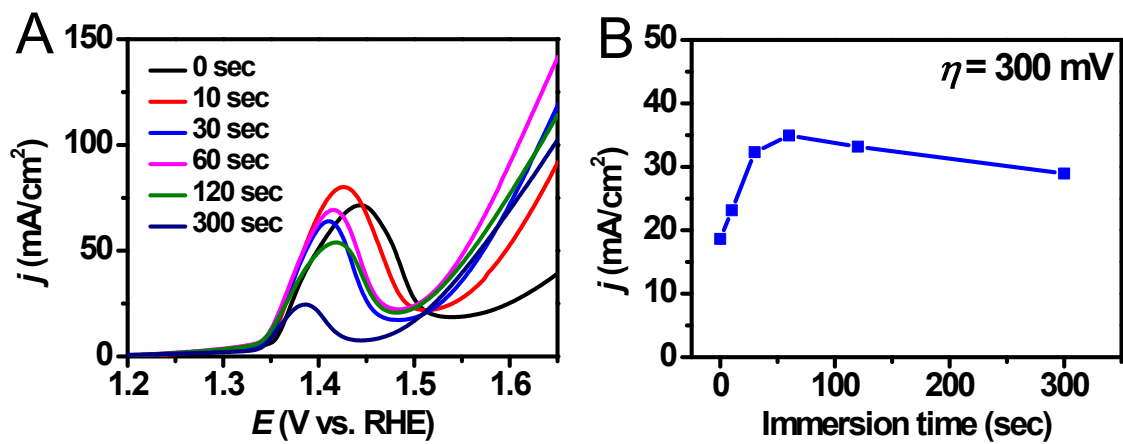


**Figure S11.** Optimization of Fe-doping of Ni:Cu(OH)<sub>2</sub>. The Ni:Cu(OH)<sub>2</sub> NWs electrode was immersed into a solution of 10 mM Fe<sup>3+</sup> for different times. LSV curves (A) and summarized current densities vs. immersion time at an overpotential of 300 mV (B). All electrochemical measurements were carried out in 1 M KOH at a scan rate of 20 mV/s with *iR* compensation.

**Table S1.** Elemental compositions as taken from the XPS peak fit.

<b>Electrode</b>	<b>Oxygen</b>	<b>Copper</b>	<b>Iron</b>	<b>Nickel</b>
<b>Cu(OH)<sub>2</sub> NWs</b>	68.6	31.4	-	-
<b>Fe:Cu(OH)<sub>2</sub> NTs</b>	63.7	1.9	34.4	-
<b>Ni:Cu(OH)<sub>2</sub> NWs</b>	70.0	3.4	-	26.6
<b>Ni:Fe:Cu(OH)<sub>2</sub> NTs</b>	70.8	2.1	4.5	22.6
<b>Ni:Fe:Cu(OH)<sub>2</sub> NTs after electrolysis</b>	73.2	1.4	4.8	20.6
<b>Fe:Ni:Cu(OH)<sub>2</sub> NWs</b>	72.7	1.8	4.2	21.3

**Table S2.** Results of ICP-OES measurements of Ni:Fe:Cu(OH)<sub>2</sub> NTs for Cu, Fe and Ni.

Element	Atomic ratio (%)
Copper	73.50
Iron	5.46
Nickel	21.04

**Table S3.** Comparison of Fe:Cu(OH)<sub>2</sub> NTs with Cu(OH)<sub>2</sub> NWs and other iron-based OER electrocatalysts in alkaline solutions.

Electrocatalyst	Substrate	Electrolyte	Current density (mA/cm <sup>2</sup> )	$\eta$ (mV)	Tafe I slope	Refs
<b>Fe:Cu(OH)<sub>2</sub> NTs</b>	Cu foil	1 M KOH	10	380	40	<b>This work</b>
<b>Cu(OH)<sub>2</sub> NWs</b>	Cu foil	0.1 M NaOH	10	430	86	[1]
<b>Fe(OH)<sub>3</sub>:Cu(OH)<sub>2</sub></b>	Cu foam	1 M KOH	10	365	42	[2]
<b>FeO<sub>x</sub></b>	FTO	0.1 M KOH	10	400	-	[3]
<b>Steel S235*</b>	Self-standing	0.1 M KOH	2	347	59	[4]
<b>FeO<sub>x</sub>H<sub>y</sub></b>	Au/Ti	1 M KOH	1	350	43	[5]
<b>Fe<sub>2</sub>O<sub>3</sub></b>	Carbon cloth	1 M KOH	10	420	-	[6]

\*consisting of Fe<sub>2</sub>O<sub>3</sub>, FeO(OH), MnO(OH), and Mn<sub>2</sub>O

**Table S4.** Comparison of Ni:Fe:Cu(OH)<sub>2</sub> NT with other NiFeO<sub>x</sub>-based OER electrocatalysts in alkaline solutions.

Electrocatalyst	Substrate	Electrolyte	Current density (mA/cm <sup>2</sup> )	$\eta$ (mV)	Tafe l slope	Refs
<b>Ni:Fe:Cu(OH)<sub>2</sub> NTs</b>	Cu foil	1 M KOH	100	320	32	<b>This work</b>
<b>Fe-doped NiO</b>	Au/QCM*	0.5 M KOH	10	297	37	[7]
<b>Fe-doped NiOOH</b>	Au	0.1 M KOH	10	~360	-	[8]
<b>NiFe-LDH</b>	Pyrolytic	1 M KOH	10	280	47	[9]
<b>NiFe-LDH</b>	Glassy carbon	1 M KOH	10	347	40	[10]
<b>NiFe-hydroxide</b>	Planar Au	1 M KOH	120	300	33	[11]
<b>NiFe<sub>0.52</sub>O<sub>x</sub></b>	Glassy carbon	1 M KOH	10	330	97	[12]
<b>NiFe-LDH</b>	Glassy carbon	1 M KOH	10	320	31	[13]
<b>NiFe<sub>0.4</sub>O<sub>x</sub></b>	FTO	0.1 M KOH	5	370	26	[14]

\*Quartz Crystal Microbalance

## SUPPLEMENTARY REFERENCES

1. C. C. Hou, W. F. Fu and Y. Chen, *ChemSusChem*, 2016, **9**, 2069-2073.
2. C. C. Hou, C. J. Wang, Q. Q. Chen, X. J. Lv, W. F. Fu and Y. Chen, *Chem. Commun.*, 2016, **52**, 14470-14473.
3. B. C. M. Martindale and E. Reisner, *Adv. Energy Mater.*, 2016, **6**, 1502095.
4. H. Schafer, K. Kupper, J. Wollschlager, N. Kashaev, J. Hardege, L. Walder, S. Mohsen Beladi-Mousavi, B. Hartmann-Azanza, M. Steinhart, S. Sadaf and F. Dorn, *ChemSusChem*, 2015, **8**, 3099-3110.
5. M. S. Burke, S. Zou, L. J. Enman, J. E. Kellon, C. A. Gabor, E. Pledger and S. W. Boettcher, *J. Phys. Chem. Lett.*, 2015, **6**, 3737-3742.
6. Y. Yan, B. Y. Xia, X. M. Ge, Z. L. Liu, A. Fisher and X. Wang, *Chem. Eur. J.*, 2015, **21**, 18062-18067.
7. K. Fominykh, P. Chernev, I. Zaharieva, J. Sicklinger, G. Stefanic, M. Doblinger, A. Muller, A. Pokharel, S. Bocklein, C. Scheu, T. Bein and D. Fattakhova-Rohlfing, *ACS Nano*, 2015, **9**, 5180-5188.
8. D. Friebel, M. W. Louie, M. Bajdich, K. E. Sanwald, Y. Cai, A. M. Wise, M. J. Cheng, D. Sokaras, T. C. Weng, R. Alonso-Mori, R. C. Davis, J. R. Bargar, J. K. Norskov, A. Nilsson and A. T. Bell, *J. Am. Chem. Soc.*, 2015, **137**, 1305-1313.
9. B. M. Hunter, J. D. Blakemore, M. Deimund, H. B. Gray, J. R. Winkler and A. M. Muller, *J. Am. Chem. Soc.*, 2014, **136**, 13118-13121.
10. F. Song and X. Hu, *Nat. Commun.*, 2014, **5**, 4477.
11. A. S. Batchellor and S. W. Boettcher, *ACS Catal.*, 2015, **5**, 6680-6689.

12. L. J. Zhou, X. Huang, H. Chen, P. Jin, G. D. Li and X. Zou, *Dalton Trans.*, 2015, **44**, 11592-11600.
13. M. Gong, Y. Li, H. Wang, Y. Liang, J. Z. Wu, J. Zhou, J. Wang, T. Regier, F. Wei and H. Dai, *J. Am. Chem. Soc.*, 2013, **135**, 8452-8455.
14. R. D. Smith, M. S. Prevot, R. D. Fagan, S. Trudel and C. P. Berlinguette, *J. Am. Chem. Soc.*, 2013, **135**, 11580-11586.